



Effect of ligand substituents on supramolecular self-assembly and electrochemical properties of copper(II) complexes with benzoylhydrazones: X-ray crystal structures and cyclic voltammetry

Dariusz Matoga*, Janusz Szklarzewicz, Wojciech Nitek

Faculty of Chemistry, Jagiellonian University, Ingardena 3, 30-060 Kraków, Poland

ARTICLE INFO

Article history:

Received 16 December 2011

Accepted 5 February 2012

Available online 11 February 2012

Keywords:

Copper
Complex
Hydrazone
Supramolecular
Substituent
Voltammetry

ABSTRACT

Complexation of copper(II) with a series of hetero-donor chelating Schiff bases (HLL^R) of *para*-substituted benzhydrazides (with R = OH, NO₂, CH₃O, Cl and *tert*-butyl substituents) and acetone affords mononuclear [Cu(LL^R)₂] molecules: **1** [Cu(anbh₂)₂] (R = NO₂); **2** [Cu(ahbh₂)₂] (R = OH); **3** [Cu(ambh₂)₂] (R = CH₃O); **4** [Cu(acbh₂)₂] (R = Cl); and **5** [Cu(atbh₂)₂] (R = *tert*-butyl). Single-crystal X-ray diffraction results for **2–5** reveal their various supramolecular architectures including 1D and 2D dimensionalities. A detailed analysis of crystal structures allows to gain insight into intermolecular interactions accountable for self-assembly into different networks as well as for various physicochemical properties of the compounds. The major interactions include O–H···N hydrogen bonds (**2**) as well as CH···N and axial Cu···O (**3**); π···π stacking (**4**) and van der Waals CH···C interactions (**5**). All compounds are characterized by elemental analyses; IR and UV–Vis spectroscopy as well as magnetic susceptibility and cyclic voltammetry measurements. Electrochemical studies reveal the dependence of [Cu(LL^R)₂]/[Cu(LL^R)₂][–] reduction potentials on substituents of benzoylhydrazone ligands.

© 2012 Elsevier Ltd. All rights reserved.

1. Introduction

The construction of coordination polymers through crystal engineering is an important field of chemistry with tremendous potential in the development of functional materials. The applications where such polymers may be used include, for instance electronic, magnetic and optoelectronic devices, advanced nanocomposites or biological sensors [1–7]. In this wide class of materials, porous metal–organic frameworks (MOFs), incorporating metals and organic ligands, give rise to a considerable and constantly increasing interest among researchers mostly due to their further promising applications in gas storage and catalysis [5–10]. MOFs are compounds that extend ‘infinitely’ into one, two or three dimensions (1D, 2D or 3D, respectively) via both covalent metal–ligand coordination as well as weaker non-covalent interactions, such as hydrogen bonding or π···π stacking. These non-covalent interactions are also important in biological systems and generally govern the physicochemical properties of molecular systems in the solid state. Undoubtedly, exploration and understanding how weak interactions work in the supramolecular systems is essential for crystal engineers who design structures, in particular those of materials based on coordination compounds with organic ligands

[5–7,11–14]. The ability of prediction of the self-assembly of small molecules in the crystalline state is still one of the most challenging topics in crystal engineering.

In the field of metal–organic frameworks, copper(II) complexes, exhibiting Jahn–Teller distortion, have recently emerged as attractive building blocks offering weak axial binding and coordination versatility [15,16]. Among various organic ligands used in the construction of porous copper coordination polymers, incorporation of Schiff-base metal complexes into channels’ walls of a well-defined porous framework still belongs to a rarity [17–19]. The pioneering synthesis of such materials has been described in the group of Kitagawa who used a ‘metalloligand’ concept with carboxylate substituted *N,N*-phenylenebis(salicylideneimine) [18]. Recently also a supramolecular lamellar structure of copper(II) Schiff-base complex was reported with relevance to enantioselective recognition and separation [19]. Schiff bases themselves and their complexes are also known to self-assemble only through supramolecular interactions, forming defined pores in the crystalline state as well as showing high surface areas and selective gas uptake [20,21].

We recently became interested in coordination polymers based on copper(II) Schiff-base complexes that may exhibit porous and/or conducting properties. As a line of this study we were investigating a series of *ortho*-hydroxybenzoyl hydrazones that have been shown to act as bridging ligands and to form interesting unusual single-chain electropolymerizable copper–organic backbones [22]. For comparison, it appeared attractive to study analogous copper

* Corresponding author. Tel.: +48 12 6632223; fax: +48 12 6340515.

E-mail address: matoga@chemia.uj.edu.pl (D. Matoga).

benzoylhydrazone systems with a series of *para*-substituents (including hydroxy group), potentially capable of forming supramolecular structures through various intermolecular interactions. The position of substituents in benzoylhydrazonate ligands has been chosen intentionally in this study as favourable for perpendicular arrangements of complexes that potentially could result in porous supramolecular networks. These complexes could also potentially become useful building blocks either as metalloligands (linkers) or as nodes (connectors) in the crystal engineering of polymeric frameworks. In spite of their attractiveness as building blocks for the construction of advanced materials, hydrazone ligands and their copper(II) complexes are also interesting as potential chemotherapeutic agents since analogous systems were found to exhibit antitumor and antibacterial activities [23–28].

In this work we report on the synthesis, X-ray crystal structures as well as spectroscopic and electrochemical properties of a series of copper(II) complexes with *para*-substituted hydrazone ligands. A detailed analysis of crystal structures is presented and the intermolecular interactions accountable for the self-assembly into different supramolecular networks as well as for various physicochemical properties of the compounds, are discussed.

2. Materials and methods

Copper(II) acetate monohydrate was synthesized according to published method [29]. All other chemicals and solvents were of analytical grade (Aldrich, Lach-ner, POCh, Polmos) and were used as supplied. Carbon, hydrogen and nitrogen were determined using an Elementar Vario MICRO Cube elemental analyzer. Solid samples for IR spectroscopy were compressed as KBr pellets and the IR spectra were recorded on a Bruker EQUINOX 55 FT-IR spectrophotometer. Electronic absorption spectra were measured with a Shimadzu UV-3600 UV-Vis-NIR spectrophotometer. Diffuse reflectance spectra were measured in BaSO₄ pellets with BaSO₄ as a reference using Shimadzu 2101PC equipped with ISR-260 attachment. Magnetic susceptibility measurements were carried out at room temperature on a Sherwood Scientific Magway MSB MK1 balance. In magnetic moments calculations corrections for diamagnetism were not used. Cyclic voltammetry measurements were carried out in DMSO with [Bu₄N]PF₆ (0.10 M) as the supporting electrolyte using Pt working and counter and Ag/AgCl reference electrodes on an AUTOLAB/PGSTAT 128N Potentiostat/Galvanostat. Cyclic voltammograms were obtained under argon at room temperature. $E_{1/2}$ values were calculated from the average anodic and cathodic peak potentials, $E_{1/2} = 0.5(E_a + E_c)$. The redox potentials were calibrated versus ferrocene, which was used as an internal potential standard for measurements to avoid the influence of liquid junction potential; the final values are reported versus ferrocenium/ferrocene couple.

2.1. Syntheses

The approach to synthesize copper benzoylhydrazone complexes utilizes a condensation reaction between acetone and a series of *para*-substituted benzoylhydrazides. The list of formed hydrazones HLL^R that were used as templates in the reaction with copper(II) acetate to give [Cu(LL^R)₂] complexes **1–5**, is presented in Fig. 1.

2.1.1. Synthesis of [Cu(anbhz)₂] (**1**)

4-Nitrobenzhydrazide (362 mg, 2.00 mmol) and acetone (140 μ L, 10.0 mmol) were dissolved in EtOH (40 mL) and heated under reflux for approx. 10–15 min. [Cu(O₂CCH₃)₂·H₂O] (200 mg, 1.00 mmol) was then added and the heating under reflux of the resultant suspension was continued for approx. 15 min. Greenish-grey precipitate of **1** was filtered off, washed thrice with small

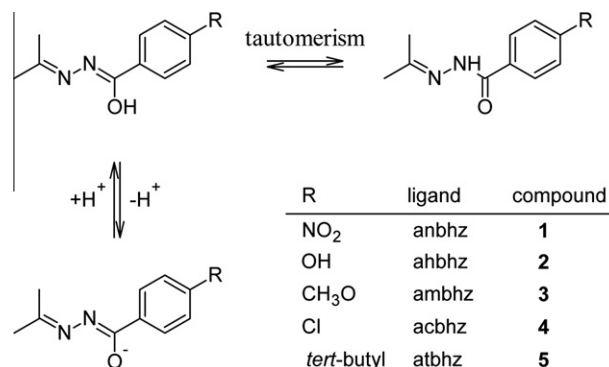


Fig. 1. Keto-enol tautomerism and reversible deprotonation of substituted benzoylhydrazones utilized as templates in the syntheses.

amount of cold EtOH and dried in air at room temperature. Yield: 0.435 g; 86.3%. *Anal. Calc.* for C₂₀H₂₀N₆O₆Cu: C, 47.67; H, 4.00; N, 16.68. Found: C, 47.04; H, 3.98; N, 16.53%. IR (KBr, cm⁻¹): $\nu_{\text{CN(imine)}}$ 1596s, 1618s, $\nu_{\text{CO(enolate)}}$ 1269 m, $\nu_{\text{sym(nitro)}}$ 1335vs, $\nu_{\text{asym(nitro)}}$ 1563vs. UV-Vis (solid state) λ , nm: 500–700broad, 420sh, 371, 272. Magnetic moment: $\mu_{\text{ef}} = 1.7 \mu_{\text{B}}$.

2.1.2. Synthesis of [Cu(ahbhz)₂]·0.5H₂O (2·0.5H₂O)

The synthetic procedure was analogous to that of **1** except that 4-hydroxybenzhydrazide (304 mg, 2.00 mmol) was used instead of 4-nitrobenzhydrazide. Yield: 0.272 g; 59.8%. *Anal. Calc.* for C₂₀H₂₃N₄O_{4.5}Cu: C, 52.80; H, 5.10; N, 12.31. Found: C, 52.81; H, 4.90; N, 12.13%. IR (KBr, cm⁻¹): $\nu_{\text{CN(imine)}}$ 1598s, 1610vs, $\nu_{\text{CO(enolate)}}$ 1243s, $\nu_{\text{CO(phenolic)}}$ 1279s. UV-Vis (solid state) λ , nm: 500–700broad, 428, 283. UV-Vis [DMSO solution: λ , nm (ϵ , dm³ mol⁻¹ cm⁻¹): 730broad (60), 420sh, 290sh. Magnetic moment: $\mu_{\text{ef}} = 1.7 \mu_{\text{B}}$. Golden-green crystals of **2** suitable for single-crystal X-ray diffraction were obtained after recrystallization from DMSO.

2.1.3. Synthesis of [Cu(ambhz)₂]·0.5H₂O (3·0.5H₂O)

The synthetic procedure was analogous to that of **1** except that 4-methoxybenzhydrazide (332 mg, 2.00 mmol) was used instead of 4-nitrobenzhydrazide. Yield: 0.359 g; 74.3%. *Anal. Calc.* for C₂₂H₂₇N₄O_{4.5}Cu: C, 54.70; H, 5.63; N, 11.60. Found: C, 54.84; H, 5.42; N, 11.60%. IR (KBr, cm⁻¹): $\nu_{\text{CN(imine)}}$ 1590s, 1609s, $\nu_{\text{CO(enolate)}}$ 1265m, $\nu_{\text{CO(methoxy)}}$ 1245s, 1309 m. UV-vis (solid state) λ , nm: 500–700broad, 420sh, 280. Magnetic moment: $\mu_{\text{ef}} = 1.5 \mu_{\text{B}}$. Dark green crystals of **3** suitable for single-crystal X-ray diffraction were obtained after recrystallization from THF/DMF mixture.

2.1.4. Synthesis of [Cu(acbhz)₂]·0.5H₂O (4·0.5H₂O)

The synthetic procedure was analogous to that of **1** except that 4-chlorobenzhydrazide (341 mg, 2.00 mmol) was used instead of 4-nitrobenzhydrazide. Yield: 0.460 g; 93.5%. *Anal. Calc.* for C₂₀H₂₁Cl₂N₄O_{2.5}Cu: C, 48.84; H, 4.30; N, 11.39. Found: C, 48.96; H, 4.14; N, 11.33%. IR (KBr, cm⁻¹): $\nu_{\text{CN(imine)}}$ 1588s, 1615 m $\nu_{\text{CO(enolate)}}$ 1267 m. UV-Vis (solid state) λ , nm: 500–700broad, 420sh, 274. UV-Vis [DMSO solution: λ , nm (ϵ , dm³ mol⁻¹ cm⁻¹): 688broad (60), 280sh. Magnetic moment: $\mu_{\text{ef}} = 1.8 \mu_{\text{B}}$. Dark green crystals of **4** suitable for single-crystal X-ray diffraction were obtained after recrystallization from DMSO.

2.1.5. Synthesis of [Cu(atbhz)₂] (**5**)

The synthetic procedure was analogous to that of **1** except that 4-*tert*-butylbenzhydrazide (384 mg, 2.00 mmol) was used instead of 4-nitrobenzhydrazide. Yield: 0.180 g; 34.2%. *Anal. Calc.* for C₂₈H₃₈N₄O₂Cu: C, 63.91; H, 7.28; N, 10.65. Found: C, 63.39; H, 7.18; N, 10.50%. IR (KBr, cm⁻¹): $\nu_{\text{CN(imine)}}$ 1584s, 1625 m, $\nu_{\text{CO(enolate)}}$

1267s, $\nu_{\text{CH(terbutyl)}}$ 2964s, 2903 m, 2867 m. UV–Vis (solid state) λ , nm: 710sh, 604, 420sh, 281. UV–Vis [DMSO solution: λ , nm (ϵ , $\text{dm}^3 \text{mol}^{-1} \text{cm}^{-1}$): 674broad (60), 280sh. Magnetic moment: $\mu_{\text{eff}} = 1.5 \mu_{\text{B}}$. Dark green crystals of **5** suitable for single-crystal X-ray diffraction were obtained after recrystallization from DMF.

2.2. Crystallographic data collection and structure refinement

The crystals of **2–5** suitable for X-ray analysis were selected from the materials prepared as described in Section 2. Intensity data for **5** were collected on Oxford Diffraction SuperNova dual source diffractometer with an Atlas electronic CCD area detector using Mova microfocuss Mo K α radiation source ($\lambda = 0.71073 \text{ \AA}$). Intensity data for **2–4** were collected on a Nonius Kappa CCD diffractometer using graphite monochromated Mo K α radiation ($\lambda = 0.71073 \text{ \AA}$). The crystal data, details of data collection and structure refinement parameters are summarized in Table 1. The positions of most atoms for all structures were determined by direct methods, other non-hydrogen atoms were located on difference Fourier maps. All non-hydrogen atoms were refined anisotropically using weighted full-matrix least-squares on F^2 . Hydrogen H7 (**2**) was identified on difference Fourier maps and refined with geometrical restraints. All other hydrogen atoms bonded to carbons were included in the structure factor calculations at idealized positions. In the structure of **5** there are electron density peaks which are not arranged in any chemically meaningful molecule. It seems that they could be associated with the strongly disordered DMF molecule. Unfortunately all attempts to model this molecule and its disorder have not given satisfactory results. The structures were solved using SIR-97 and refined by SHELXL program [30,31].

3. Results and discussion

3.1. X-ray crystal structures

Compounds **2–5** possess four-coordinate copper centers that are surrounded by two bidentate hydrazones bound in the *trans*-N,O mode. The centers in **2–4** adopt square planar geometry (with deviations from an ideal square induced by chelate bite angles of

80.7–80.9°) whereas compound **5** exhibits an intermediate geometry between square planar and tetrahedral (Fig. 2). The dihedral angle between the two coordination planes defined by O(8)–Cu(1)–N(10) and O(28)–Cu(1)–N(30) is 28.5°. Crystal structures of analogous mononuclear *trans*-CuN₂O₂ four-coordinate complexes with Schiff bases derived from salicyl- or hydroxynaphthalenecarboxaldehydes and bulky amines (1-ethylpropylamine, 1-naphthylethylamine, 1-phenylethylamine or cycloamines) also exhibited mostly geometries that are intermediate between square planar and tetrahedral; dependent on steric effects of substituents at the nitrogen atom [32–37]. Bond angles in complexes **2–5** support the square planar (**2–4**) and intermediate (**5**) geometries (Table 2), with O–Cu–Oⁱ ranging from 180 (**2–4**) to 156.2° (**5**) and N–Cu–Nⁱ angles from 180 (**2–4**) to 168.2° (**5**). The Cu–O and Cu–N bonds in **2, 3, 4** and **5** have similar lengths and are in the same range as those reported for salicyloylhydrazone copper(II) complexes, i.e. Cu–O distances are in the range of 1.88–1.91 Å, and Cu–N distances have values between 1.99 and 2.05 Å [22]. The values of other bond lengths are also comparable to those found for salicyloylhydrazone copper(II) complexes.

The various packing patterns of compounds **2–4** in the solid state are illustrated in Figs. 3 and 4. The supramolecular structure of complex **2** is based on strong O–H \cdots N hydrogen bonds between hydroxo substituents and nitrogen atoms of hydrazonate ligands from adjacent complexes (Fig. 3). The observed hydrogen-bond distances are: O7 \cdots N11 2.804 Å, H7 \cdots N11 2.044 Å, O7–H7 0.763 Å; and the hydrogen-bond angle is 174° (O7–H7 \cdots N11). The complexes are arranged interchangeably perpendicular to each other forming herringbone layers, thus validating our assumption on favourable perpendicular arrangements introduced with *para*-substituents of the ligands. Interestingly, the supramolecular layers formed are 2D rectangular grids with approximately 8 \times 11 Å cavities. Unfortunately however, these layers do not assemble into porous network since the lack of proper interlayer separator makes adjacent layers decrease the cavity dimension, as is shown on the example of two layers in Fig. 3.

The solid state structure of complex **3** can be described as supramolecular 2D layers parallel to the *bc* plane that are stacked along the *a* axis, and includes a combination of CH \cdots N and Cu \cdots O interactions, the latter involving hydrazonate methoxy substituents whose oxygen atoms can be treated as occupying axial

Table 1
Crystal data and structure refinement parameters for **2–5**.

	2	3	4	5
Empirical formula	C ₂₀ H ₂₂ N ₄ O ₄ Cu	C ₂₂ H ₂₆ N ₄ O ₄ Cu	C ₂₀ H ₂₀ Cl ₂ N ₄ O ₂ Cu	C _{31.5} H ₃₈ N ₄ O ₂ Cu
Formula weight	445.97	474.01	482.84	568.20
Crystal size (mm)	0.25 \times 0.20 \times 0.06	0.14 \times 0.14 \times 0.03	0.60 \times 0.25 \times 0.10	0.51 \times 0.28 \times 0.08
Crystal system	monoclinic	monoclinic	monoclinic	triclinic
Space group	P2 ₁ /c	P2 ₁ /c	P2 ₁ /c	P $\bar{1}$
<i>a</i> (Å)	6.7090(3)	7.8720(4)	15.3700(4)	7.777(5)
<i>b</i> (Å)	14.6870(7)	9.3920(5)	4.66400(10)	11.610(5)
<i>c</i> (Å)	11.9480(5)	15.7670(8)	16.8490(4)	17.410(5)
α (°)	90.00	90.00	90.00	85.957(5)
β (°)	123.369(3)	112.788(3)	122.097(2)	80.031(5)
γ (°)	90.00	90.00	90.00	77.191(5)
<i>V</i> (Å ³)	983.21(8)	1074.72(10)	1023.21(4)	1508.9(12)
<i>Z</i>	2	2	2	2
<i>T</i> (K)	293(2)	293(2)	293(2)	293(2)
<i>D</i> _{calc} (mg/m ³)	1.506	1.465	1.567	1.251
μ (mm ⁻¹)	1.146	1.053	1.353	0.757
Reflections measured	16,607	8679	14,840	9734
Reflections unique	2241	2450	2311	6243
Reflections observed [<i>I</i> > 2 σ (<i>I</i>)]	1930	1589	1955	4242
<i>R</i> indices [<i>I</i> > 2 σ (<i>I</i>)]				
<i>R</i>	0.0628	0.0417	0.0347	0.0488
<i>wR</i> ₂	0.1145	0.0905	0.0916	0.1207
<i>S</i>	1.303	0.978	1.091	0.980

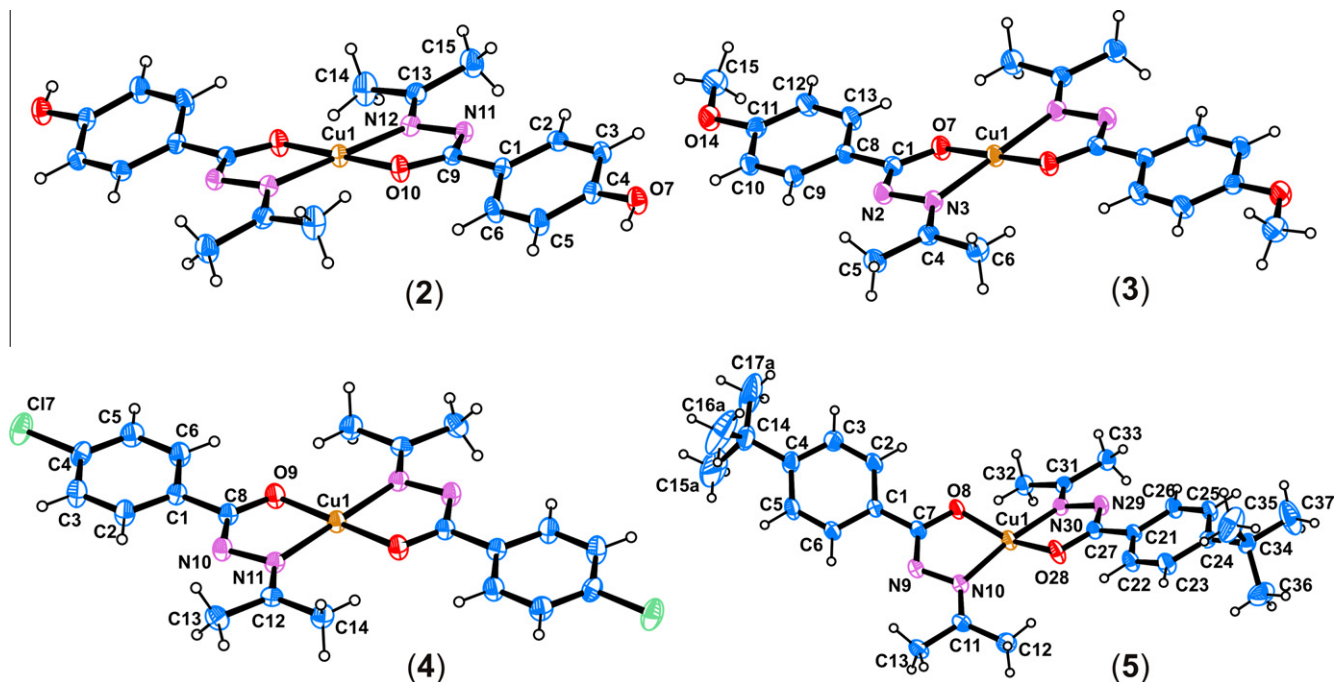


Fig. 2. Single-crystal X-ray structures of [Cu(ahbhz)₂] (**2**), [Cu(ambhz)₂] (**3**), [Cu(acbhz)₂] (**4**) and [Cu(atbhz)₂] (**5**) showing the atom labeling scheme and 50% displacement ellipsoids.

Table 2

Selected bond lengths (Å) and angles (°) for [Cu(ahbhz)₂] (**2**), [Cu(ambhz)₂] (**3**), [Cu(acbhz)₂] (**4**) and [Cu(atbhz)₂] (**5**) with estimated standard deviations in parentheses. Unless otherwise stated, all bond lengths and angles involve atoms within five-membered rings containing copper.

	2	3	4	5
<i>Bond lengths</i>				
Cu–O	1.880(3)	1.9006(18)	1.8916(14)	1.895(2) 1.904(2)
Cu–N	2.044(2)	2.037(2)	2.0396(15)	1.996(2) 2.004(2)
C–O	1.291(4)	1.301(3)	1.292(3)	1.311(3) 1.299(3)
C–N	1.306(4)	1.298(3)	1.301(2)	1.310(3) 1.300(3)
N–N	1.419(5)	1.421(3)	1.410(2)	1.403(3) 1.408(3)
N–C(outside the ring)	1.289(5)	1.298(3)	1.296(2)	1.283(3) 1.295(3)
<i>Bond angles</i>				
O–Cu–O ⁱ	180.00(16)	180	180	156.25(10)
N–Cu–N ⁱ	180.0(2)	180	180	168.18(9)
O–Cu–N	80.68(10)	80.89(8)	80.92(6)	81.90(9) 81.29(9)
O–Cu–N ⁱ	99.32(10)	99.11(8)	99.08(6)	100.62(9) 101.12(9)

positions of a Jahn–Teller elongated octahedral complex (Fig. 4). The adjacent stacks of complexes are held together by pairs of weak CH \cdots N interactions along the [010] direction (H \cdots N distance is 2.660 Å) as well as the axial coordination with the Cu1–O14 distance 3.050 Å that links complexes along the [001] direction and is most probably responsible for the poor solubility of the compound.

In the crystal structure of **4** planar copper complexes are stabilized by $\pi\cdots\pi$ face-to-face stacking interactions along the [010] direction forming infinite 1D supramolecular chains. The complexes are arranged along the [001] lattice vector with alternating stacking planes that are perpendicular to each other (Fig. 4). The closest observed intermetallic Cu \cdots Cu distance is 4.664 Å.

Tetrahedrally distorted complexes **5** form chains along the [100] direction that alternate along the *b* axis (Fig. 5). The complexes are stabilized by weak van der Waals CH \cdots C interactions. The lack of specific intermolecular interactions such as observed for complexes **2**, **3** and **4** seems to be accountable for the tetrahedral distortion of compound **5**. Chains of complexes, related by a translation along the *c* axis, are separated by layers of strongly disordered molecules.

3.2. Cyclic voltammetry

The redox properties of all copper(II) complexes **1–5** have been studied by cyclic voltammetry (CV). The cyclic voltammograms were recorded at various scan speeds (100–1000 mV s⁻¹) over the range from –1500 to 1000 mV (versus Ag/AgCl) in DMSO. All recorded voltammograms were performed with the cell-off mode (zero current flow) before and after measurements so as not to generate any new species near the working electrode. We have found, that independently on single or multiscan mode or else starting potential there were no significant changes in the number of peaks observed. All narrow ranges were scanned in the multiscan mode in order to verify appearing signals as reproducible and stable ones as well as to obtain good quality curves. At the end of analysis for each compound, ferrocene was added as an internal potential standard.

The electrochemical data are summarized in Table 3 and the representative voltammograms for all complexes are presented in Fig. 6. One distinct quasireversible or reversible electrochemical process is observed for each compound within the DMSO window. These redox waves appear at relatively low potentials and are attributable to a ligand-centered process involving the imino group of the enol form of the coordinated ligands. The reduction of the imine group to the radical anion has been previously reported for Schiff-base complexes [38]. Here, the noteworthy feature is the reversibility or quasireversibility of the reduction which is due to Cu(II) stabilized anion radicals. Apart from the distinct signals, presented for all complexes in Fig. 6, we have also observed some

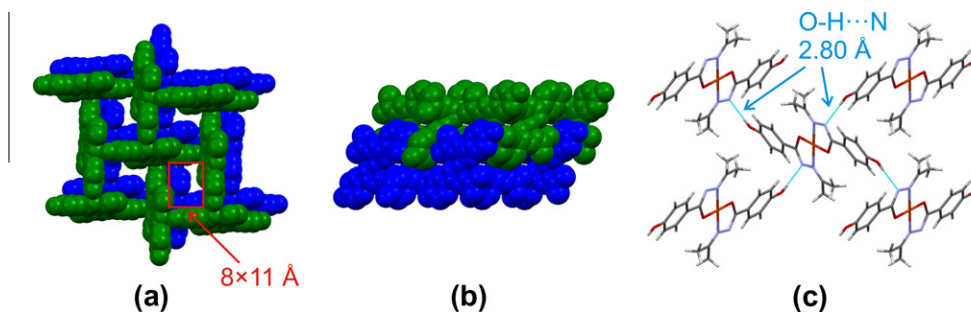


Fig. 3. Single-crystal X-ray crystal structure of $[\text{Cu}(\text{ahbhz})_2]$ (**2**), illustrating the packing pattern with 2D supramolecular layers containing rectangular cavities, and viewed in a spacefill mode (a) along a^* and (b) along b and (c) perspective along a . Separate layers are indicated in blue and green and hydrogen atoms are omitted for clarity. Hydrogen bonds (pale blue lines) are additionally shown and viewed along a (c). (For interpretation of the references to colour in this figure legend, the reader is referred to the web version of this article.)

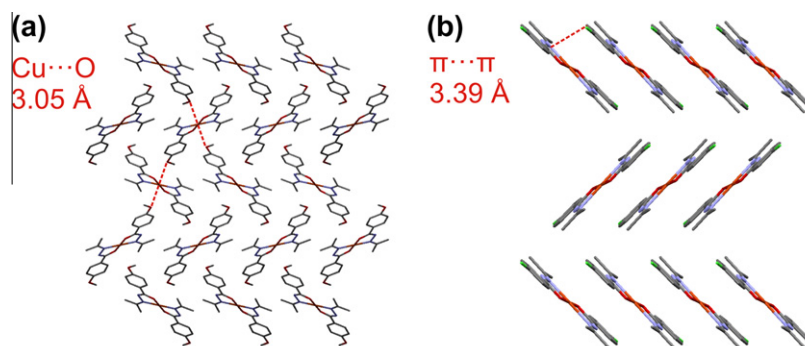


Fig. 4. Single-crystal X-ray crystal structures of (a) $[\text{Cu}(\text{ambhz})_2]$ (**3**) and (b) $[\text{Cu}(\text{acbhz})_2]$ (**4**) illustrating the packing patterns and viewed along a (a) and along a^* (b). Hydrogen atoms are omitted for clarity. Selected intermolecular separations are indicated as red dashed lines. (For interpretation of the references to colour in this figure legend, the reader is referred to the web version of this article.)

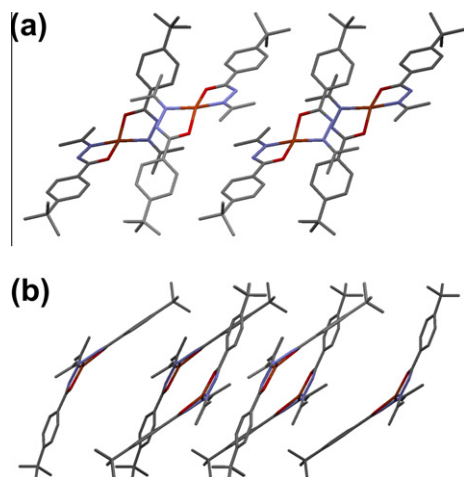


Fig. 5. Single-crystal X-ray crystal structure of $[\text{Cu}(\text{atbhz})_2]$ (**5**), illustrating the packing pattern, and viewed (a) along a , (b) along the $[1-10]$ direction. Hydrogen atoms and disordered molecules are omitted for clarity.

peaks at a more positive potential but these have been found to be ill-defined, of low intensity, and often elusive when narrow-range scans have been performed. The only reliable signal, attributed to a copper-centered process, has been observed as a reversible wave at $E_{1/2} = -0.12$ V (versus Fc^+/Fc) for compound **1**. Analogous waves have not been observed for the rest of complexes. Most probably copper-centered reductions of these complexes lead to their instant decomposition.

Table 3

Selected electrode potentials $E_{1/2}$ (V vs. Fc^+/Fc) and peak-to-peak separations ΔE for the anodic and cathodic processes exhibited by the complexes **1–5** in DMSO solutions (measurements carried out at 200 mV/s).

Complex	$E_{1/2}$	ΔE	Comments
1	-1.52	0.10	Reversible
2	-1.17	0.26	Reversible
3	-1.23	0.13	Reversible
4	-1.02	0.30	Quasireversible
5	-1.11	0.38	Quasireversible

The reduction potentials become considerably less negative in the following order of benzoylhydrazonate *para*-substituents: nitro (**1**) < methoxy (**3**) < hydroxy (**2**) < *tert*-butyl (**5**) < chloro (**4**). Taking into account the electro-donating and -withdrawing character of the substituents expressed by Hammett σ_p parameters, the order of decreasing electro-withdrawing character (decreasing σ_p) is: nitro ($\sigma_p = 0.78$; **1**) < chloro ($\sigma_p = 0.23$; **4**) < *tert*-butyl ($\sigma_p = -0.20$; **5**) < methoxy ($\sigma_p = -0.27$; **3**) < hydroxy ($\sigma_p = -0.37$; **2**) [39]. Clearly the two orders differ from each other; compounds with *tert*-butyl (**5**) and chloro substituents (**4**) are the easiest to reduce in the whole series whereas they both are characterized by relatively high Hammett σ_p parameter. The redox potentials for the rest of compounds (with oxygen containing substituents) are in agreement with substituent electro-withdrawing character. Most probably the breakdown of this trend can be explained by: (a) bulky substituents of complex **5** leading to its tetrahedrally distorted geometry, different from the rest of the complexes with a square planar geometry; as well as (b) by different solvation pattern for complexes **4** and **5** in comparison with the other compounds. The latter effect may be

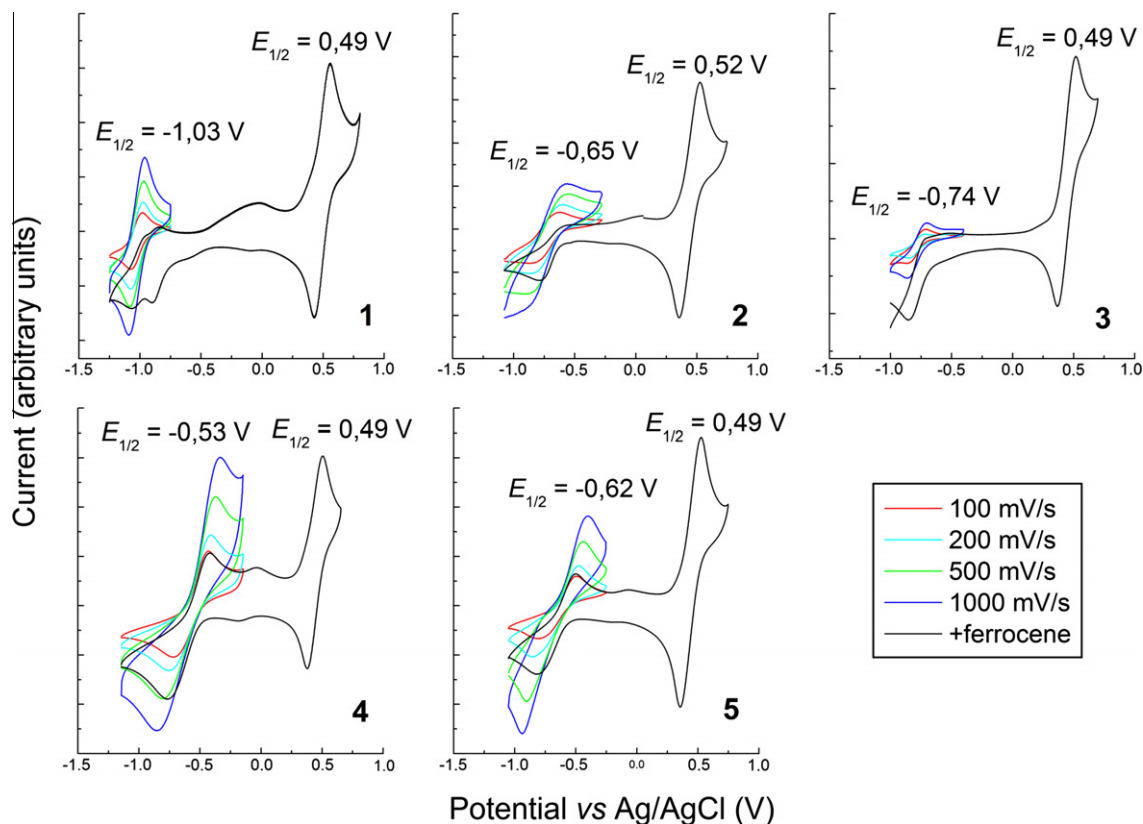


Fig. 6. Cyclic voltammograms recorded for complexes 1–5 in DMSO solutions. Experimental potential values are measured vs. Ag/AgCl at 200 mV s⁻¹.

associated with a coordination of DMSO that is an aprotic solvent with Lewis base character. Such coordination in complexes 1–3 is hindered by the presence of substituents with oxygen donors. This explanation is also supported by the fact that complexes 4 and 5 are freely soluble in DMSO whereas compounds 1–3 are poorly soluble. Another feature that distinguishes complexes 4 and 5 from the rest of the copper compounds is the quasireversible character of the electrochemical reduction. It indicates a relatively slow electron transfer in comparison with applied scan rates, that may be the result of the presence of a steric hindrance in the proximity of imine groups.

4. Conclusion

In conclusion, the synthesis of compounds 1–5 has shown the potential for various substituents of aromatic hydrazone ligands as diverse supramolecular synthons in crystal engineering. These groups engage in intermolecular interactions yielding a variety of supramolecular architectures for copper(II) complexes. This series has the potential to be greatly expanded with different hydrazone ligands and the use of other metal centres, such as for instance Ni(II), Co(II), Mn(II) whose complexes may become useful building blocks in the construction of coordination polymers including MOFs, and this is currently under study.

Acknowledgements

The research was carried out with the equipment purchased thanks to the financial support of the European Regional Development Fund in the framework of the Polish Innovation Economy Operational Program (Contract No. POIG.02.01.00-12-023/08).

Appendix A. Supplementary data

CCDC 858982, 858983, 858984 and 858985 contain the supplementary crystallographic data for 2, 3, 4 and 5, respectively. These data can be obtained free of charge via <http://www.ccdc.cam.ac.uk/conts/retrieving.html>, or from the Cambridge Crystallographic Data Centre, 12 Union Road, Cambridge CB2 1EZ, UK; fax: +44 1223 336 033; or e-mail: deposit@ccdc.cam.ac.uk.

References

- [1] G.R. Whittell, M.D. Hager, U.S. Schubert, I. Manners, *Nature Mat.* 10 (2011) 176.
- [2] V.A. Friese, D.G. Kurth, *Curr. Opin. Colloid Interface Sci.* 4 (2009) 81.
- [3] D.G. Kurth, M. Higuchi, *Soft Matter* 2 (2006) 915.
- [4] X. Lin, J. Jia, X. Zhao, K.M. Thomas, A.J. Blake, G.S. Walker, N.R. Champness, P. Hubberstey, M. Schroder, *Angew. Chem., Int. Ed.* 45 (2006) 7358.
- [5] G.R. Desiraju (Ed.), *Crystal Design: Structure and Function*, vol. 7, John Wiley & Sons, Ltd., Chichester, England, 2003.
- [6] C. Janiak, J.K. Vieth, *New J. Chem.* 34 (2010) 2366.
- [7] C. Janiak, *Dalton Trans.* (2003) 2781.
- [8] S. Kitagawa, R. Kitaura, S. Noro, *Angew. Chem., Int. Ed.* 43 (2004) 2334.
- [9] A.K. Cheetham, C.N.R. Rao, R.K. Feller, *Chem. Commun.* (2006) 4780.
- [10] B. Moulton, M.J. Zaworotko, *Chem. Rev.* 101 (2001) 1629.
- [11] G.R. Desiraju, *Angew. Chem., Int. Ed.* 46 (2007) 8342.
- [12] G.F. Swiegers, in: J.A. McCleverty, T.J. Meyer (Eds.), *Comprehensive Coordination Chemistry II*, vol. 1, Elsevier, Oxford, UK, 2004, Chap. 1.43, p. 747.
- [13] C.B. Aakeröy, A.M. Beatty, in: J.A. McCleverty, T.J. Meyer (Eds.), *Comprehensive Coordination Chemistry II*, vol. 1, Elsevier, Oxford, UK, 2004, Chap. 1.37, p. 679.
- [14] Y.E. Alexeev, B.I. Kharisov, T.C. Hernández García, A.D. Garnovskii, *Coord. Chem. Rev.* 254 (2010) 794.
- [15] S. Noro, *Phys. Chem. Chem. Phys.* 12 (2010) 2519.
- [16] S. Noro, K. Fukuhara, K. Kubo, T. Nakamura, *Cryst. Growth Des.* 11 (2011) 2379.
- [17] S. Kitagawa, S. Noro, T. Nakamura, *Chem. Commun.* (2006) 701.
- [18] R. Kitaura, G. Onoyama, H. Sakamoto, R. Matsuda, S. Noro, S. Kitagawa, *Angew. Chem., Int. Ed.* 43 (2004) 2684.
- [19] G. Yuan, C. Zhu, W. Xuan, Y. Cui, *Chem. Eur. J.* 15 (2009) 6428.
- [20] M. Mastalerz, M.W. Schneider, I.M. Opped, O. Presly, *Angew. Chem., Int. Ed.* 50 (2011) 1046. and references therein.

- [21] J.H. Chong, S.J. Ardakani, K.J. Smith, M.J. MacLachlan, *Chem. Eur. J.* 15 (2009) 11824.
- [22] D. Matoga, J. Szklarzewicz, R. Gryboś, K. Kurpiewska, W. Nitek, *Inorg. Chem.* 50 (2011) 3501.
- [23] E.W. Ainscough, A.M. Brodie, A.J. Dobbs, J.D. Ranford, J.M. Waters, *Inorg. Chim. Acta* 267 (1998) 27.
- [24] E.W. Ainscough, A.M. Brodie, W.A. Denny, G.J. Finlay, S.A. Gothe, J.D. Ranford, *J. Inorg. Biochem.* 77 (1999) 125.
- [25] S.C. Chan, L.L. Koh, P.H. Leung, J.D. Ranford, K.Y. Sim, *Inorg. Chim. Acta* 236 (1995) 101.
- [26] D.K. Johnson, T.B. Murphy, N.J. Rose, W.H. Goodwin, L. Pickart, *Inorg. Chim. Acta* 67 (1982) 159.
- [27] L. Pickart, W.H. Goodwin, W. Burgua, T.B. Murphy, D.K. Johnson, *Biochem. Pharmacol.* 32 (1983) 3868.
- [28] A.A. Aruffo, T.B. Murphy, D.K. Johnson, N.J. Rose, V. Schomaker, *Inorg. Chim. Acta* 67 (1982) L25.
- [29] J. Supniewski, *Preparatyka nieorganiczna*, PWN, Warszawa, 1985. p. 693.
- [30] A. Altomare, G. Cascarano, G. Giacobozzo, A. Guagliardi, M.C. Burla, G. Polidori, M. Camalli, *J. Appl. Cryst.* 27 (1994) 435.
- [31] G.M. Sheldrick, *Acta Crystallogr., Sect. A* 64 (2008) 112.
- [32] J.M. Fernandez-G, C. Ausun-Valdes, E.E. Gonzalez-Guerrero, R.A. Toscano, *Z. Anorg. Allg. Chem.* 633 (2007) 1251.
- [33] A.L. Iglesias, G. Aguirre, R. Somanathan, M. Parra-Hake, *Acta Crystallogr., Sect. E* 62 (2006) o390.
- [34] A.L. Iglesias, G. Aguirre, R. Somanathan, M. Parra-Hake, *Polyhedron* 23 (2004) 3051.
- [35] J.M. Fernandez-G, F.A. Lopez-Duran, S. Hernandez-Ortega, V. Gomez-Vidales, N. Macias-Ruvalcaba, M. Aguilar-Martinez, *J. Mol. Struct.* 612 (2002) 69.
- [36] M. Aguilar-Martinez, R. Saloma-Aguilar, N. Macias-Ruvalcaba, R. Cetina-Rosado, A. Navarrete-Vazquez, V. Gomez-Vidales, A. Zentella-Dehesa, R.A. Toscano, S. Hernandez-Ortega, J.M. Fernandez-G, *Dalton Trans.* (2001) 2346.
- [37] A.D. Garnovskii, I.S. Vasil'chenko, *Russ. Chem. Rev.* 71 (2002) 943.
- [38] P. Gili, M.G. Martin Reyes, P. Martin Zarza, M.F.C. Guedes da Silva, Y.-Y. Tong, A.J.L. Pombeiro, *Inorg. Chim. Acta* 255 (1997) 279.
- [39] C. Hansch, A. Leo, R.W. Taft, *Chem. Rev.* 91 (1991) 165.